Webology (ISSN: 1735-188X)
Volume 18, Number 6, 2021

The Automatic Diagnosis Systems For Detecting Glaucoma In Fundus Images Using Fusion GLCM And CNN Techniques

K.Subha[1] , Dr. S.Kother Mohideen[2]

[1]Reg.No 18221252162003, Research Scholar, Department of IT, Sri Ram Nallamani Yadava College of Arts & Science (Affiliation of Manonmaniam Sundaranar University) Tenkasi, Tamilnadu – 627804, India.

[2]Associate Professor & Head, Department of Information Technology, Sri Ram Nallamani Yadava College of Arts & Science Tenkasi, Tamilnadu – 627804, India.

Abstract

The automated detection of optical disc in the retinal fundus images is gaining more attention by ophthalmologists. Optical disc detection plays a crucial role in retinal image processing for the identification of various fundus structures and eye disorders. The proposed study first determines how human perception functions for optical disc detection using a bottom-up visual focus paradigm since human visual vision has not been extensively studied for optical disc detection and an attempt to acquire data analytics based on eyes. Accurate early identification could prevent eyesight problems. Glaucoma can be identified using several categorization techniques, and the severity of the condition is evaluated in retinal images. Novel computations are developed to distinguish between and categorise the different stages of glaucoma. The affectability, specificity, and exactness of the execution measurements need to be examined. The precision of our method was 95.81%. Additionally, it is anticipated that the proposed developed algorithm will aid doctors in early diagnosis of diabetic retinopathy.

Keywords: Glaucoma detection, optic disc, Pre-trained CNNs and Classification.

1. Introduction

Nearly 250 million people worldwide are affected by diabetes at the moment. In the event that a person has diabetes, their blood glucose level is elevated and their retina is harmed. This causes a visual deficiency or vision malfunction. Glaucoma is a frequent eye condition associated with diabetes that impairs vision. One in four of those who have the same sort of glaucoma, which affects about 4.1 million people, experience vision loss. According to the National Eye Organization, glaucoma is the primary cause of vision impairment and vision impedance in adults

between the ages of 20 and 74. It is also the cause of poor vision in diabetics. High blood pressure can harm the blood vessels that supply the retina, which results in glaucoma. This issue may result in internal eye disease, hazy vision, and completely impaired eyesight. Typically, the disorder may damages the optic nerve and blocks blood flow.

1.1 PROBLEM STATEMENT

One of the most common retinal issues among people with chronic illnesses and the main factor in blindness is glaucoma. Glaucoma can be effectively treated with early detection and ongoing examination. The automated detection of Glaucoma from computerised fundus images is necessary to prevent vision loss. It will highly reduce the time taken for examination of the illness.

Exudates harm the retina in patients with glaucoma's eyes. Exudates in the retina harm the blood vessels and result in leakage of protein and lipid from the bloodstream. The patients will become blind if the exudates reach the macular region of the retina.The existing works lack efficiency in the identification of glaucoma process in digital fundus images.

2. Literature survey

To find out which methods were most frequently employed in the glaucoma diagnosis from photographs, we examined through the literature. The MA, haemorrhages, hard exudates, and soft exudates were classified using the statistical classifiers k-nearest neighbour, Bayesian, and Mahalanobis [1]. A region-growing algorithm uses fundus pictures to highlight potential lesions. The Mahalanobis classifier produces the greatest results as statistical classifiers divide candidate lesions into four categories. The sensitivity values are stated [2], but the specificity numbers are not mentioned.

An automated framework is essential for computerised image analysis to identify Glaucoma in retinal fluoresce in angiographic images. It is regarded as a successful tool for the early diagnosis of diabetic retinal degeneration in glaucoma [3]. These techniques work by removing blood vessels from the retinal image, classifying the entire image, and then identifying whether or not circular objects are caused by glaucoma. The benefit is that it reduces the quantity of incorrect discovery MAs, making progress in execution seem. An innovative method using neural networks and thresholding to detect haemorrhages and glaucoma in colour retinal pictures is employed in[4]. By using a region-growing algorithm, the hard exudates are discovered. With the suggested technique, sensitivity of 80.21% and specificity of 70.66% were achieved.

To suggest a method for analysing colour fundus images for glaucoma, haemorrhages, and exudates. Color fundus images are preprocessed in order to make use of local differentiation upgrading and colour standardisation techniques. For classification, fake neural networks are employed [5]. To determine MA, exudates, locale developing computation, versatile escalation thresholding, and edge improvement administrators are used. With the improvements to the suggested strategy, further advancements may be obtained [6].

An innovative approach to combat Glaucoma with colour fundus images. To distinguish Glaucoma, preprocessing techniques and potential extractors are used. The candidates are categorised using a machine learning method, which is also utilised to choose the feature subset selection procedure. The technique now performs better [7]. The complexity of the suggested method is the limitation.

A novel method for glaucoma detection in fundus photographs is proposed in [8]. The regular detection of diabetic retinopathy was covered in detail [8] To distinguish glaucoma damage, a successful and quick-working technique is used. The first illustration is to depict the symptoms of diabetic retinopathy. The suggested approach is predicated on numerical morphology, object pixel classification, and associated component research [9]. For images with a resolution of 2048x1536 pixels, this suggested calculation responds in 4.8 seconds. It appears that this framework operates more quickly than existing frameworks for glaucoma detection. The framework's affectability and specificity, respectively, are 69.1% and 99.3% [10].

The colour retinal images allow for an examination of the phases of retinopathy . Here, image analysis tools are used to examine the severity of diabetic retinopathy, such as exudates, glaucoma, and hemorrhages, as well as the programmed detection of various aspects of the disease. The suggested approach is effective, and it is being carried out more quickly [11].

A framework for making a decision at the end of DR based on the quantity and placement of MAs and HAs Division is associated to enlargement, disintegration, opening, closure, reproduction, and top-hat and bottom-hat morphological alteration procedures [12]. For the purpose of finding dim injuries, the top-hat and bottom-hat distinguish upgrade methods, h-maxima change, and multilayer thresholding are used. For the localization of MAs, the framework achieves an affectability of 84.31% and a specificity of 93.63%. Additionally, it generates 95.08% specificity and 87.53% affectability [13].

The method for glaucoma detection in retinal images is developed. Early detection of glaucoma will slow the progression of diabetic retinopathy. The suggested method can more quickly identify the signs of Glaucoma and identify it in images of low quality [14].

The plan based on an outline of study to advance the discovery of glaucoma is proposed. The treatment of restorative images is still grappling with the problem of reliable glaucoma detection in advanced fundus images [15]. Preprocessing techniques and candidate extractors are combined with internal Glaucoma locators, to be more precise. The proposed approach for this task is tested on the publicly available Messid or database because the location of Glaucoma is crucial when reviewing diabetic retinopathy, even though promising AUC 0.90 with 0.01 instability is achieved in a DR/non-DR-type classification based on the presence or absence of Glaucoma [16].

The use of a fundus camera in conjunction with a programmed screening framework to

identify diabetic retinopathy is discussed. Spatial features are used for location, and a fake neural network is used to classify the images [17]. The specialists will be helped by programmed screening to quickly and accurately identify the state of the silence. The extent of exudates, glaucoma, neovasculatures, etc. is quantified and categorically identified from fundus photographs [18].

A modified colour auto-correlogram that has been spectrally adjusted for DR images has higher dimensionality. The categorization assignment using the suggested include is carried out using a multi-class, multiple-instance learning system [19]. Wide-ranging testing, including comparisons with several cutting-edge picture classification methods, have been carried out, and the results indicate that the suggested method is promising because it outperforms other strategies by a significant margin [20].

Proposed System

The fundus images can be separated into distinct regions, and each region has a relationship with histogram equalization. The barrier separating the regions is removed through bilinear interpolation. Low contrast values enable the identification of the tiny blood arteries. Finally, the relative colour that was extracted from the image is classified using the suggested Convolutional Neural Network (CNN).

Histogram Equalization

Histogram equalisation is a technique that can be used to change the concentrated values of the images and enhance differentiation. The yield point histogram is then aligned with another designated histogram at that point. The contrast of the fundus image is improved via histogram equalisation. The histogram is frequently changed to do this. The fundus image is upgraded using a differentiated improvement approach, and the histogram essentially depicts the occurrence event of each grey level, from 0 to 255.The histogram equalization is

$$r_k = \frac{n_k}{N} \quad (1)$$

where

n_k is the intensity level

Nis the total number of pixels in image

Let fundus image can be represented by m' and pixel intensities of integer may be

ranging from 0 to L-1

$$\rho_n = \frac{\text{number of pixels with intensity n}}{\text{Total number of pixels}} \qquad n = 0,1,\ldots\ldots, L-1 \tag{2}$$

where

L is the intensity values

ρ is normalized histogram

As a result, the fundus image is improved and is more likely to become bright. The reassignment of intensity pixel values to the already-existing ones results in the creation of a uniform intensity distribution. Contrast of the filtered image is improved using contrast enhancement.

Walter-Klein Preprocessing Method

The Walter-Klein preprocessing approach uses changes in grey level to enhance fundus picture differentiation. The input fundus images show a connection between these alterations. Brightness and differentiation of the fundus images are improved by using grey level modification.

They are characterised as by applying negative modification to fundus images

$$S = L-1-r \tag{3}$$

The log transformation can be defined as

$$s = clogr + 1 \tag{4}$$

Were, s,r is pixel value of input and output image

c is a constant

These power law transformations can be given by the expression

$$s = Cr^r \tag{5}$$

Principal Component Analysis (PCA)

The core of the study is a strong measurable strategy. This method can be used to identify high measurement designs. PCA is used for pattern recognition and face compression. In pattern recognition problems, the preparation images are stored in a key component frame, and the information is then used to determine whether a hidden dataset and the stored information are similar or dissimilar. In the successful discovery of optical plates, PCA is used. The determination of the optic disc's location is a part of the localization phase of the proposed research.

PCA consists of three stages.

- The Eigen vectors are calculated for training images.
- The fundus image is positioned in the space designated by the Eigen vectors, and
- The distance between the fundus image and the projection is calculated.

The fundus images are part of the training set of the proposed research. The training set's optic disc has been cropped. Sub-images of intensity are shrunk by L*L pixels and normalised.
The training set's vector dimension is L2.

The training set's average vector is calculated using

$$\Psi = \frac{1}{M} \sum_{i-1}^{m} T_i \quad (6)$$

The average vector of training set is

$$C = \frac{1}{M} \sum_{i-1}^{m} T_{i\varphi} \quad T_{i=} \quad WW^T \quad (7)$$

$i\varphi$

where

W is a matrix

φ_i is the mean centered image

In PCA, a set of images are required for training images. Let N be the total number of images used in the training image with n*n dimensions.

Let mn_i and mx_i are the minimum and maximum values in training image set as follows

$$mn_i = min[I_i] \quad (8)$$

$$mx_i = max[I_i - mn_i] \quad (9)$$

Normalized training image is as follows

$$I^n_i = \frac{I_i - mn_i}{mx_i} 255 \quad (10)$$

In training image, the mean is computed by following equation

$$M = \frac{1}{N} \sum_{i=1}^{N} I_i \quad (11)$$

The mean image is subtracted from the normalized training image as shown below

$$I^{nm}_{i} = I^{n}_{i} - m \quad (12)$$

The required data formed by PCA is given by the following equations

$$D = \{\{fI^{nm}_{i}[K, I] \forall 1 \leq i \leq N\}[2, N], I^{nm}_{i}[n, n]\} \quad (13)$$

The data D has a dimension and co variance matrix is formed by

$$C_{D} = \frac{DT}{N} \quad (14)$$

A feature vector is formed by
Feat vect = eigen value [c]
Feat vect is computed by $Finaldat_1$ and sum_1 and is given by

$$Finaldat_1 = \text{Feavec}. D^T$$

$$Sum_1 = \sum_{p=1}^{N} \sum_{q=1}^{n_2} Finaldat_1^2[p, q] \quad (15)$$

The error is defined by

$$error = Sum_1 - Sum_2 \quad (16)$$

The sum_2 is defined by

$$Sum_2 = \sum_{} \sum_{} Finaldat_2^2[p, q] \quad (17)$$

p□1 q□1

The $Finaldat_2$is defined by

$$Finaldat_2 = (Featvec[1]^T . \{patch\})$$

This approach explains the training photos and aids in determining how similar the unknown image resembles the images in the training set.

Convolutional Neural Network

The CNN demonstration, often known as snakes, is used in computer vision and picture-handling software. The protest's limits are accurately found by CNN's demonstration. To separate the fundus images or retinal images and identify the optic plate, CNN is used. This method is based on fundus photographs to show the division processes more clearly.

The snakes, or active contour model, use three different techniques.

i. Traditional snakes
ii. Geometric Active contour (Level set method)
iii. Gradient vector flow (GVF) method

i. Traditional snakes

This method involves moving the curve through the image domain for a given energy function, where the energy depends on both internal and external forces.

It is given by

$$E_{snake} = E_{internal} + E_{external} \quad (18)$$

Finally, the segmented image is acquired and computed using

$$\emptyset_t = V(x,t)|\nabla\emptyset| \quad (19)$$

ii. Gradient Vector Flow(GVF) method

This method is used for better segmentation and the GVF field is calculated from the image.

$$Q = \iint \mu V + |\nabla f|^2 |V - \nabla f|^2 dx \quad (20)$$

GVF method is enhanced using

- Adaptive balloon force
- Dynamic GVF force

Adaptive balloon force is calculated by

$$Fp(S) = k.n(s) \quad (21)$$

In dynamic GVF force, it is noted that the field vector direction changes at the ellipse boundary.

3. Result and Discussion

The classification parameters used in WEKA were the standard ones for each classifier, and the validation method used was k-fold cross-validation (with k = 10). We used the 873 images from the progression set for these tests.

Table 1 Number of images within the improvement.

Database	Healthy	Non-Pathological	Total
DRISTI	30	67	97
RIM-sample-1	117	42	159
RIM- sample -2	257	203	460
RIM- sample -3	86	75	161
Total	490	387	877

(a) (b) (c)

Fig. 2. Sample database of retinal images: (a) sample set of HRF; (b) sample set ofJSIEC; and (c) sample set of ACRIMA.

Table 2 Number of images within the improvement set.

Database	Healthy	Glaucomatous	Total
HRF	15	14	29
JSIEC	53	14	67
ACRIMA	307	397	707
total	375	425	803

(a) (b) (c) (d) (e)

Input Retinal Images

(a) (b) (c) (d) (e)

Pre-Processed Images

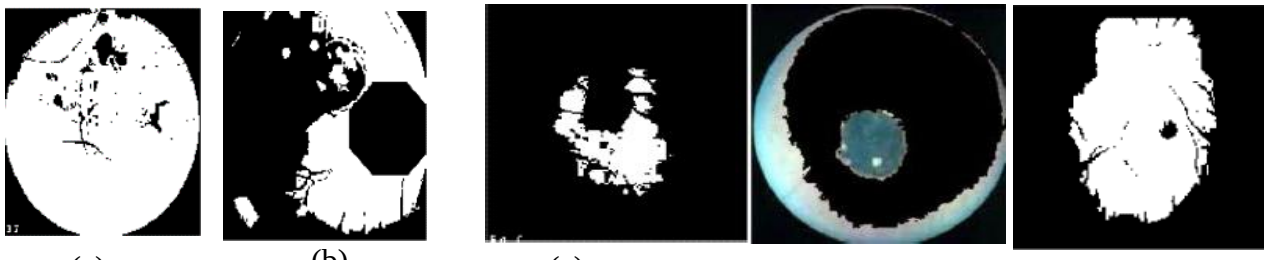

(a) (b) (c) (d) (e)

Segmented Images

Fig. 3. Preprocessing and Segmentation results of the various iris image.

Figure 3 shows the restored outcome of the preprocessing and splitting of various iris images.

Table 3 Result for Unusual Pictures Include Extraction

Sample Images	Mean (db)	SD (db)	RMS	Variance (db)	Energy (J)
HRF	22.3	22.8	5.1	23.0	13.7
JSIEC	32.4	65.9	7.8	23.9	23.8
ACRIMA	37.0	70.8	7.6	34.1	43.5
DRISTI	39.8	73.8	8.4	45.9	55.1

Table 4 Kappa gotten for each set of highlights and for each classifier within the improvement set of pictures.

Techniques	**Kappa (%)**		
	SVM	**MLP**	**Random Forest**
LBP	0.00%	51%	48%
GLCM	61.05%	70%	65%
HOG	55%	45%39%	51%
Tamura	36.12%	48%	41%
GLRLM	25.98%	22%	49%
Morphology	6.1%	66%	32%
CNN-AlexNet	63.88%	62%	59%
CNN-CaffeNet	60.45%	61%	61%
CNN-Vgg-f	61.02%	65%	62%
CNN-Vgg-m	63.97%	62%	62%
CNN-Vgg-s	62%	60%	64%
CNN-Vgg-16	57%	62%	60%
CNN-Vgg-19	67.2%	61%	62%

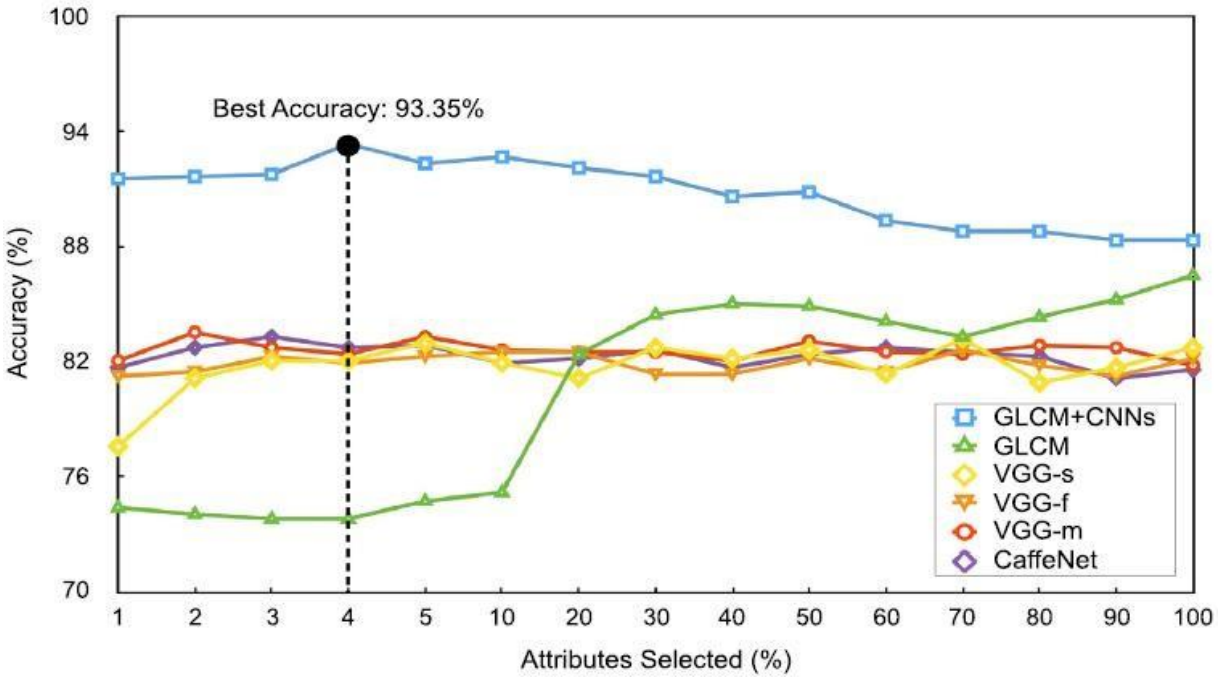

Fig. 4. Performance measures of various classifier Accuracy

However, by joining them, the outcome was completely improved, reaching an accuracy of 93.35% with only 4% of the properties, or 659 qualities from a possible 16,469.

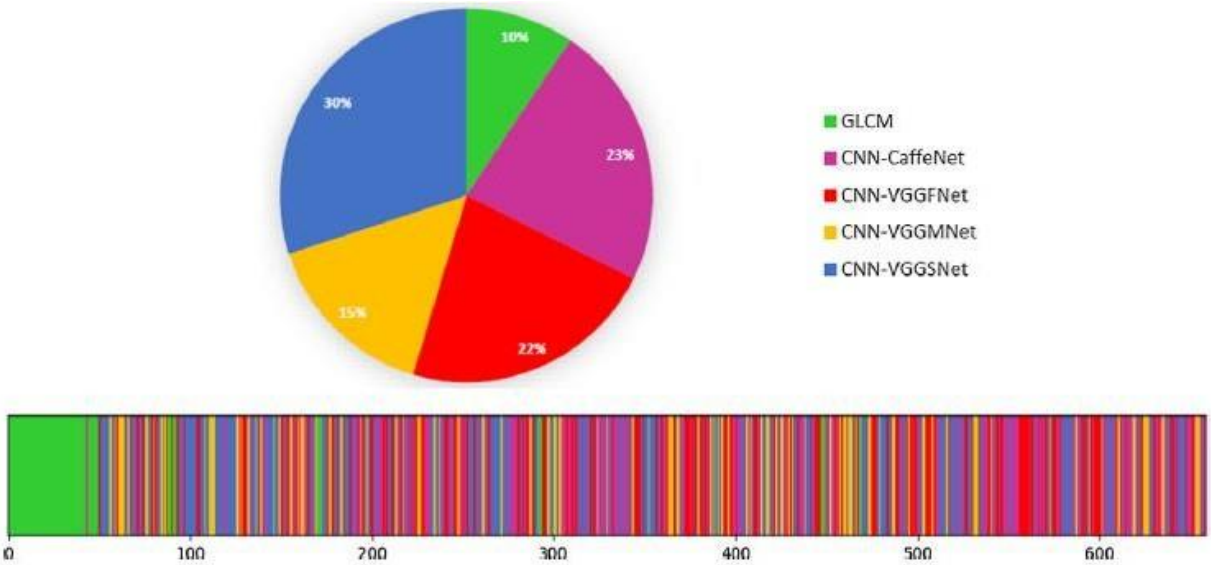

Fig. 5. Composition of the proposed descriptor.

Table 5 Different classifier feature value.

Techniques	A(%)	K(5)	P(%)	AUC(%)
GLCM	85.23	73.12	85.78	94.99
CNN+CaffeNet	83	65.46	82.8	90.32
CNN+VGGFNet	81.7	64.32	83.31	88.7
CNN+VGGMNet	85.9	67.5	83.7	89.8
CNN+VGGSNet	83.4	64.9	82.88	90
GLCM+CNN	96.02	87.32	92.89	97.98

A heuristic search of the best parameters was used to obtain the results shown in the last line of Table 5. We connected it to the HRF, JSIEC, and ACRIMA databases with the parameters defined before to demonstrate that the suggested technique works well in images of various databases.

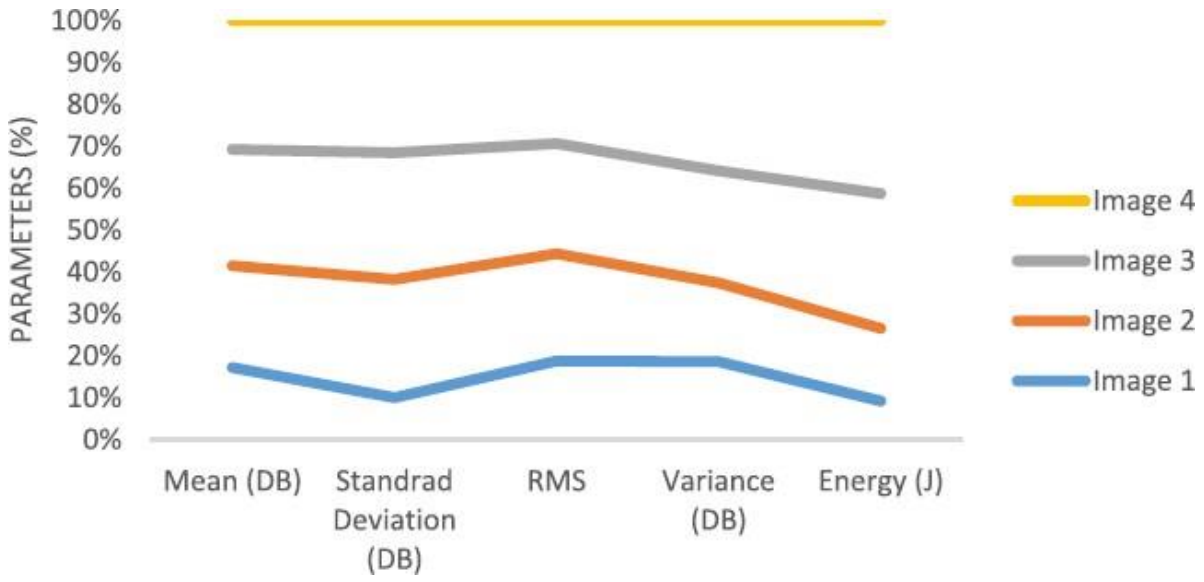

Fig. 6. The Comparison chart for abnormal images.

According to Fig. 6, the highlight extraction within the retinal infection region is compared using metrics such as standard deviation, RMS, fluctuation, and the vitality of these highlights for the outcome of classification standard disease discovery using CNN calculation..

4. Conclusion

A number of Computer Aided Diagnosis (CAD) systems have been created to use retinal scans to identify glaucoma in its early stages. The main focus of CAD systems is on nodule detection and identification. There are no CAD systems available to determine the stage of glaucoma.

The accuracy in segmenting the nodule is one of the main shortcomings of current CAD systems. The primary predictor of survival at the time of the affected region's investigation is its stage, and

this defines the course of treatment. When compared to other testing-training phases, the 80-20% phase produces the best accuracy (93.35%).

References

1. Wang, Yu, and Shan Shan. "Accurate disease detection quantification of iris based retinal images using random implication image classifier technique." Microprocessors and Microsystems 80 (2021): 103350.
2. Claro, Maila, Rodrigo Veras, Andre Santana, Flavio Araujo, Romuere Silva, Joao Almeida, and Daniel Leite. "An hybrid feature space from texture information and transfer learning for glaucoma classification." Journal of Visual Communication and Image Representation 64 (2019): 102597.
3. Casson, Robert J., Glyn Chidlow, John PM Wood, Jonathan G. Crowston, and Ivan Goldberg. "Definition of glaucoma: clinical and experimental concepts." Clinical & experimental ophthalmology 40, no. 4 (2012): 341-349. Casson, Robert J., Glyn Chidlow, John PM Wood, Jonathan G. Crowston, and Ivan Goldberg. "Definition of glaucoma: clinicaland experimental concepts." Clinical & experimental ophthalmology 40, no. 4 (2012): 341- 349.
4. R. Bock, J. Meier, G.Michelson, L. G. Nyl, and J. Hornegger, “Classifyingglaucoma with image-based features from fundus photographs,”Proc. of DAGM, pp. 355–364, 2017.
5. Cheng, Jun, Fengshou Yin, Damon Wing Kee Wong, Dacheng Tao, and Jiang Liu. "Sparse dissimilarity-constrained coding for glaucoma screening." IEEE Transactions on Biomedical Engineering 62, no. 5 (2015): 1395-1403.
6. Yadav, Deepti, M. Partha Sarathi, and Malay Kishore Dutta. "Classification of glaucoma based on texture features using neural networks." In 2014 Seventh International Conference on Contemporary Computing (IC3), pp. 109-112. IEEE, 2014.
7. Hu, Man, Chenghao Zhu, Xiaoxing Li, and Yongli Xu. "Optic cup segmentation from fundus images for glaucoma diagnosis." Bioengineered 8, no. 1 (2017): 21-28.
8. Ramani, R. Geetha, Lakshmi Balasubramanian, and Shomona Gracia Jacob. "Automatic prediction of Diabetic Retinopathy and Glaucoma through retinal image analysis and data mining techniques." In 2012 International Conference on Machine Vision and Image Processing (MVIP), pp. 149-152. IEEE, 2012.
9. Zhang, Ya Q., Jing Li, Liang Xu, Li Zhang, Zhen C. Wang, Hua Yang, Chang X. Chen, Xi S. Wu, and Jost B. Jonas. "Anterior visual pathway assessment by magnetic resonance imaging in normal-pressure glaucoma." Acta ophthalmologica 90, no. 4 (2012): e295-e302.
10. Yin, Fengshou, Damon Wing Kee Wong, Ying Quan, Ai Ping Yow, Ngan Meng Tan, Kavitha Gopalakrishnan, Beng Hai Lee et al. "A cloud-based system for automatic glaucoma screening." In 2015 37th Annual International Conference of the IEEE Engineering in Medicine and Biology Society (EMBC), pp. 1596-1599. IEEE, 2015.
11. Lekhana, N. P., T. C. Manjunath, and Pavithra Govindaraiah. "Development of GUI for Detection of Glaucoma using FCM and SVM." In 2018 3rd IEEE International Conference on Recent Trends in Electronics, Information & Communication Technology (RTEICT), pp.

2298-2302. IEEE, 2018.

12. Haleem, Muhammad Salman, Liangxiu Han, Jano Van Hemert, and Baihua Li. "Automatic extraction of retinal features from colour retinal images for glaucoma diagnosis: a review." Computerized medical imaging and graphics 37, no. 7-8 (2013): 581-596.
13. GeethaRamani, R., and C. Dhanapackiam. "Automatic localization and segmentation ofOptic Disc in retinal fundus images through image processing techniques." In 2014 International Conference on Recent Trends in Information Technology, pp. 1-5. IEEE, 2014.
14. R. Bock, J. Meier, L. G. Nyl, and G. Michelson, “Glaucoma risk index:Automated glaucoma detection from color fundus images,” Med. ImageAnal., vol. 14, pp. 471–481, 2010.
15. Anantha Vidya Sagar, S.Balasubramaniam and V.Chandrasekaran, “ANovel Integrated Approach using Dynamic Thresholding and EdgeDetection (IDTED) for Automatic Detection of Exudates in DigitalFundus Retinal Images”, Proc. of the International Conference on Computing: Theory and Applications, 2017, pp. 705-710.
16. Clara I. Sanchez et.al, “A novel automatic image processing algorithm fordetection of hard exudates based on retinal image analysis”, MedicalEngineering and Physics, vol. 30, pp. 350-357, 2008.
17. Agnifili, Luca, Rodolfo Mastropasqua, Paolo Frezzotti, Vincenzo Fasanella, Ilaria Motolese, Emilio Pedrotti, Angelo Di Iorio, Peter A. Mattei, Eduardo Motolese, and Leonardo Mastropasqua. "Circadian intraocular pressure patterns in healthy subjects, primary open angle and normal tension glaucoma patients with a contact lens sensor." Acta Ophthalmologica 93, no. 1 (2015): e14-e21.
18. Niwas, Swamidoss Issac, Weisi Lin, Chee Keong Kwoh, C-C. Jay Kuo, Chelvin C. Sng, Maria Cecilia Aquino, and Paul TK Chew. "Cross-examination for angle-closure glaucoma feature detection." IEEE journal of biomedical and health informatics 20, no. 1 (2015): 343- 354.
19. Pavithra, G., Anusha Tugashetti, T. C. Manjunath, and L. Dharmanna. "Investigation of primary glaucoma by CDR in fundus images." In 2017 2nd IEEE International Conference on Recent Trends in Electronics, Information & Communication Technology (RTEICT), pp. 1841-1848. IEEE, 2017.
20. Rebinth, Anisha, and S. Mohan Kumar. "A Deep Learning Approach To Computer Aided Glaucoma Diagnosis." In 2019 International Conference on Recent Advances in Energy-efficient Computing and Communication (ICRAECC), pp. 1-6. IEEE, 2019.